

Breakdown of the $Z = 8$ Shell Closure in Unbound ^{12}O and its Mirror Symmetry

D. Suzuki,^{1,2,*} H. Iwasaki,^{1,2,*} D. Beaumel,² L. Nalpas,³ E. Pollacco,³ M. Assié,² H. Baba,⁴ Y. Blumenfeld,² N. De Séréville,² A. Drouart,³ S. Franchoo,² A. Gillibert,³ J. Guillot,² F. Hammache,² N. Keeley,⁵ V. Lapoux,³ F. Maréchal,² S. Michimasa,⁶ X. Mougeot,³ I. Mukha,⁷ H. Okamura,⁸ H. Otsu,⁴ A. Ramus,² P. Roussel-Chomaz,⁹ H. Sakurai,^{4,1} J.-A. Scarpaci,² O. Sorlin,⁹ I. Stefan,² and M. Takechi⁴

¹Department of Physics, University of Tokyo, 7-3-1 Hongo, Bunkyo, Tokyo 113-0033, Japan

²Institut de Physique Nucléaire, IN2P3-CNRS, Université de Paris Sud, F-91406 Orsay, France

³CEA-Saclay, DSM/IRFU SPhN, F-91191 Gif sur Yvette Cedex, France

⁴RIKEN Nishina Center, 2-1 Hirosawa, Wako, Saitama 351-0198, Japan

⁵Department of Nuclear Reactions, The Andrzej Sołtan Institute for Nuclear Studies, ul. Hoża 69, 00-681 Warsaw, Poland

⁶CNS, University of Tokyo, RIKEN Campus, 2-1 Hirosawa, Wako, Saitama 351-0198, Japan

⁷Universidad de Sevilla, E-41012 Sevilla, Spain

⁸RCNP, Osaka University, Mihogaoka Ibaraki 567-0047, Japan

⁹GANIL, CEA/DSM - CNRS/IN2P3, Bd Henri Becquerel, BP 55027, F-14076 Caen Cedex 5, France

(Received 2 June 2009; published 9 October 2009)

An excited state in the proton-rich unbound nucleus ^{12}O was identified at 1.8(4) MeV via missing-mass spectroscopy with the $^{14}\text{O}(p, t)$ reaction at 51 AMeV. The spin-parity of the state was determined to be 0^+ or 2^+ by comparing the measured differential cross sections with distorted-wave calculations. The lowered location of the excited state in ^{12}O indicates the breakdown of the major shell closure at $Z = 8$ near the proton drip line. This demonstrates the persistence of mirror symmetry in the disappearance of the magic number 8 between ^{12}O and its mirror partner ^{12}Be .

DOI: 10.1103/PhysRevLett.103.152503

PACS numbers: 25.40.Hs, 21.10.Hw, 24.10.Eq, 27.20.+n

Symmetry and its breaking have played an important role in physics. The CP violation in particle physics led to the discovery of the third generation of quarks [1]; superconductivity of solid states is a manifestation of the gauge symmetry breaking in electron motion [2].

Mirror symmetry in atomic nuclei is a unique feature of the two-fermionic quantum system comprised of protons and neutrons. Because of the charge invariance of the nuclear force, “*mirror*” nuclei, a pair of nuclei where numbers of protons and neutrons are interchanged, show a marked similarity in their level schemes. However, the presence of the strong Coulomb field in the proton-rich mirror partner can degrade the symmetry, enhancing complex but rich aspects of the finite system.

The increasing availability of radioactive ion (RI) beams opens new possibilities to test mirror symmetry among nuclei with large isospin even beyond the drip lines. The isospin degree of freedom of the nuclear shell structure makes a sharp contrast to other quantum systems such as the quantum dots [3] and the metal clusters [4], where the electromagnetic or spatial degree of freedom is employed in manipulating the shell structure. Recent experimental studies on exotic nuclei have shown that the conventional magic numbers disappear in the neutron-rich regions at $N = 8, 20$ and 28 [5–11], and possibly in superheavy elements [12]. Theoretical works point to various underlying mechanisms in terms of the isospin-dependent part of the nuclear effective interaction [13,14], reduction of the spin-orbit potential [15], coupling to the continuum [16], and deformation [17] or clustering [18,19]. However, the

validity of the mirror symmetry of these effects at extreme conditions of isospin and binding energies remains an open question, limiting predictions for very proton-rich nuclei. The present Letter presents a study of shell quenching at $Z = 8$ in the proton-unbound nucleus ^{12}O . Mirror symmetry in the shell quenching phenomena between $^{12}_8\text{O}_4$ and its mirror partner $^{12}_4\text{Be}_8$ is investigated experimentally from the low-lying excitation properties.

We studied the structure of ^{12}O via missing-mass spectroscopy with the $^{14}\text{O}(p, t)$ reaction at 51 AMeV. The systematics of the low-lying excited states in even-even nuclei provides a sensitive probe for the evolution of the shell structure. In ^{12}Be , the anomalously low excitation energies of the 2^+ [5], 1^- [6] and 0^+ [7] excited states, clearly indicate the reduced shell gap at $N = 8$ between the p and sd shells. For ^{12}O , however, experimental difficulties have hampered establishing the level scheme. Earlier studies with the $^{16}\text{O}(\alpha, ^8\text{He})$ [20] and $^{12}\text{C}(\pi^+, \pi^-)$ [21] reactions suggested excited states at 1.1 and 1.7 MeV, respectively, while the low statistics and the lack of angular distribution data limited reliable identification. A more recent measurement of a neutron-stripping reaction with an RI-beam ^{13}O [22] only observed the ground state. The advantage of the present reaction is the sensitivity of the angular distributions to the transferred angular momentum ΔL . An observation of the characteristic distributions provides a firm confirmation of new states. Furthermore, the (p, t) reaction predominantly transfers a spin-singlet pair and populates the states with the spin-parity (J^π) of $\Delta L^{(-)\Delta L}$ when the initial state has a $J^\pi = 0^+$.

In missing-mass studies with RI beams, measurements of the energies and angles of the recoiling targetlike particles are essential to identify excited states of interest and determine the scattering angles of the reaction. The recoiling ions generally have low energies, placing a severe constraint on possible target thickness. However, the present $^{14}\text{O}(p, t)^{12}\text{O}$ reaction, which has a highly negative Q value (-31.7 MeV), occurs with a strong reduction of the momentum of the incoming beam (^{14}O) in producing the reaction product (^{12}O), which gives, instead, a relatively large momentum for the light particle (t) emitted in the forward direction. This feature enables us to use a 1-mm-thick solid hydrogen target [23] to increase the experimental yield. Together with the state-of-the-art particle detection system MUST2 [24], we realized a measurement of the (p, t) reaction, cross sections of which can be as low as several tens of μb .

The experiment was performed at the GANIL facility. The secondary ^{14}O beam at 51 AMeV was produced by fragmentation of ^{16}O at 90 AMeV on a 920-mg/cm²-thick C target located in the SISSI device [25]. The Alpha fragment separator, equipped with a 135-mg/cm²-thick Al degrader, was used to purify the fragments. The beam was delivered to the hydrogen target located at the scattering chamber of the SPEG spectrometer [26]. The beam spot on the target (P_{xy}) and incident angles (θ_{in}) were monitored by two sets of multiwire low pressure chambers, CATS [27], placed upstream of the target. The typical rms of P_{xy} (θ_{in}) was 2 mm (2.5 mrad). The time of flight, obtained as the timing difference between the radio frequency of the cyclotron and CATS, provided a clear identification of the beam. The purity (intensity) of the ^{14}O beam was around 40% (6×10^4 pps). A measurement was also performed with the degraded ^{16}O beam at 39 AMeV to obtain reference data.

The energies and angles of the recoiling tritons were measured by an array of four MUST2 telescopes [24] located 30 cm downstream of the target. Each telescope, with an active area of 10×10 cm², consisted of a 0.3-mm-thick double-sided Si strip detector (DSSD) and a 4-cm-thick 16-fold CsI calorimeter, which provided energy-loss (ΔE) and residual-energy (E) measurements, respectively. The setup covered laboratory (center-of-mass) scattering angles θ_{lab} (θ_{cm}) of 5° – 30° (10° – 160°). The acceptance of the array for the present reaction was estimated by a Monte Carlo simulation using the GEANT4 code [28], which took into account the detector geometry and the beam profile. The acceptance has a maximum value of 60% at $\theta_{\text{lab}} = 10^\circ$ – 20° ($\theta_{\text{cm}} = 30^\circ$ – 130°), while it gradually decreases toward smaller or larger angles. Particle identification of light particles was made by the ΔE - E method. The total kinetic energy (TKE) was obtained as a sum of the energy information ($\Delta E + E$), for which a correction was made based on the calculated energy loss in the target. The DSSD was divided into 256 strips in both the x and y directions, providing position information (P'_{xy}) on the

array. The emission angle θ_e of the recoiling particles was thus obtained by combining the information on the beam (P_{xy} and θ_{in}) and P'_{xy} .

Excited states in the reaction products of interest were identified using a two dimensional plot, θ_e vs TKE, for the recoiling tritons. This is demonstrated in Fig. 1(a) for the $^{16}\text{O}(p, t)$ reaction. We applied a triple coincidence with the ^{16}O beam, the recoiling tritons, and the beamlike ejectiles of either ^{14}O (for the bound states of ^{14}O) or ^{13}N (for the unbound states of ^{14}O above the proton separation energy S_p of 4.63 MeV). The ejectiles were detected by SPEG or a Si ΔE - E telescope provided by RIKEN, where the former was used to cover most forward angles up to 2° , while the latter complementarily covered larger angles from 2° to 5° [29]. In Fig. 1(a), two loci, corresponding to the 0^+ ground state (0_{gs}^+) and the first 2^+ (2_1^+) state at 6.59 MeV in ^{14}O , are evident. The excitation energy spectrum is produced based on relativistic kinematics and presented in Fig. 1(b). In addition to the two major peaks for the ground and 2_1^+ states, one can also observe a minor peak for the second 2^+ (2_2^+) state at 7.77 MeV, showing the sensitivity of the spectrum.

The θ_e vs TKE plot and the excitation energy spectrum for ^{12}O are shown in Figs. 2. Since ^{12}O is unbound for the $^{10}\text{C} + 2p$ decay, the data were obtained in coincidence with the ^{14}O beam, the recoiling tritons, and the ^{10}C ejectiles. The lower cross sections result in a worse signal-to-noise ratio in Fig. 2(a), while the energy spectrum clearly exhibits a peak at 0 MeV [Fig. 2(b)], which corresponds to the ground state of ^{12}O . One can see another peak at around 2 MeV, indicating an excited state of ^{12}O . Besides, the spectrum exhibits a broad bump centered at 5 MeV, possible origins of which are ascribed to a superposition of resonances in ^{12}O and background from other ^{14}O reactions into the $t + p + ^{10}\text{C}$ channel.

A Gaussian fit to the spectrum in Fig. 2(b) gives peak energies (E_x) of 0.0(4) and 1.8(4) MeV for the ground and excited states of ^{12}O , respectively, where the errors are dominated by the systematic error of 0.3 MeV. We assumed a constant background, determined from a fit to the data

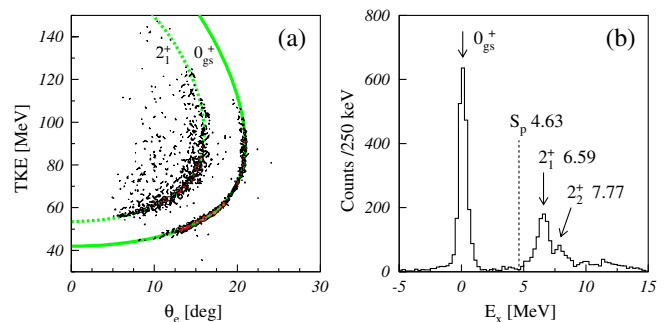


FIG. 1 (color online). (a) The θ_e vs TKE plot for the $^{16}\text{O}(p, t)$ reaction. The solid and dotted lines represent the kinematics of the reactions for the ground and first 2^+ states in ^{14}O , respectively. (b) Excitation energy spectrum of ^{14}O .

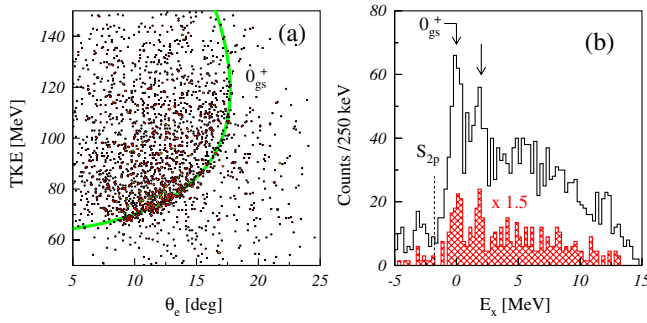


FIG. 2 (color online). (a) The θ_e vs TKE plot for the $^{14}\text{O}(p, t)$ reaction. The solid line represents the kinematics of the reaction for the ^{12}O ground state. (b) Excitation energy spectrum of ^{12}O . The dashed line indicates the $^{10}\text{C} + 2p$ decay threshold (S_{2p}) at -1.78 MeV. The red-hatched histogram shows the spectrum gated by $\theta_{\text{cm}} = 35\text{--}45^\circ$.

below 0 MeV. Peak widths were deduced to be 1.2(2) and 1.6(3) MeV FWHM for the ground and excited states, respectively. After deconvolution with the experimental resolution, which was estimated to be 1.0(5) MeV based on the $^{16}\text{O}(p, t)$ data, we obtained natural decay widths of 0.6(5) and 1.2(6) MeV for the ground and excited states, respectively. The former agrees with the previous values of 0.40(25) [20] and 0.578(205) MeV [22], while they disagree with the theoretical predictions of less than 0.1 MeV [30,31]. Note that the narrow width of the ground state ensures that the 1.8 MeV peak has a different origin. An analysis with other background forms led to similar results which vary within the errors.

Differential cross sections deduced for the observed reactions are shown in Figs. 3; vertical bars represent statistical errors only. We estimate a systematic error of 25% which stems from uncertainties in the acceptance simulation (15%) and target thickness (10%). The data were obtained by analyzing the individual spectra gated by the each angular bin. An example of the gated spectra for the $^{14}\text{O}(p, t)$ reaction is shown in Fig. 2(b). The $^{14}\text{O}(p, t)$ data at large angles of $\theta_{\text{cm}} \geq 50^\circ$ can be smaller by about a factor of 2 with different choices of the background form due to the limited statistics. The diffractive phase, characterized by the location of the peaks and dips

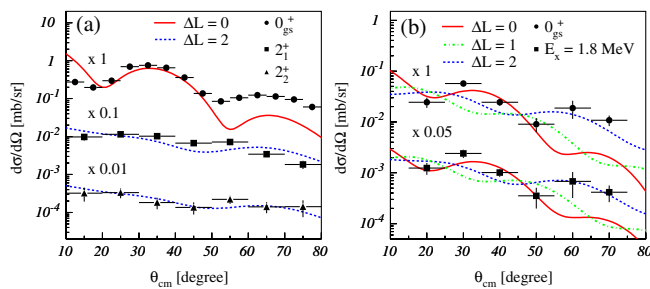


FIG. 3 (color online). Differential cross sections of the reactions (a) $^{16}\text{O}(p, t)^{14}\text{O}$ and (b) $^{14}\text{O}(p, t)^{12}\text{O}$. The experimental data are compared to the distorted-wave calculations for $\Delta L = 0$ (full), 1 (dot-dashed) and 2 (dashed lines).

in the angular distribution, offers the most reliable means of identifying ΔL . In Fig. 3(a), the $^{16}\text{O}(p, t)$ data represent characteristic phases depending on J^π . As for the $^{14}\text{O}(p, t)$ data [Fig. 3(b)], the diffractive patterns, clearly observed for the ground and 1.8 MeV states, provide convincing evidence for both states. It is further notable that the pattern of the 1.8 MeV state is almost identical to that of the ground state. This suggests $\Delta L = 0$ for the 1.8 MeV data because the ground state of even-even ^{12}O should have $J^\pi = 0^+$ to be populated by $\Delta L = 0$.

To confirm the above discussion, we performed distorted-wave calculations with the code FRESKO [32], assuming a two-neutron cluster transfer. Bound state form factors for the two-neutron cluster were similar to those of Ref. [33]. We employed global optical-model potential parameters for proton [34] and triton [35]; use of the recent GDP08 global potential [36] in the exit channel led to qualitatively similar results. As shown in Fig. 3(a), the calculations for the $^{16}\text{O}(p, t)$ reaction well reproduce the diffractive phase of the data. In Fig. 3(b), we compare the $^{14}\text{O}(p, t)$ data with calculations for $\Delta L = 0, 1$ and 2. The pattern of the $\Delta L = 1$ calculation is clearly incompatible with either angular distribution. However, while the $\Delta L = 0$ distributions most closely match the data for both states, $\Delta L = 2$ cannot be completely ruled out. We therefore determine J^π of the newly-observed state at 1.8(4) MeV to be 0^+ or 2^+ .

The evolution of the proton shell closure among neutron-deficient oxygen isotopes is studied from the systematics of the excitation energies of the low-lying states. We first plot, in Fig. 4, E_x of the first 2^+ (2_1^+) and the second 0^+ (0_2^+) states in $^{12,14,16}\text{O}$ with $Z = 8$. In ^{14}O and ^{16}O , both the 2_1^+ and 0_2^+ states are located at high excitation energies of about 6 MeV. This indicates significant effects due to the proton shell closure at $Z = 8$ as well as the neutron major (sub) shell closure at $N = 8$ ($N = 6$) for ^{16}O (^{14}O). In contrast, the 1.8 MeV state in ^{12}O illustrates an abrupt lowering of E_x , suggesting enhanced proton or neutron excitations.

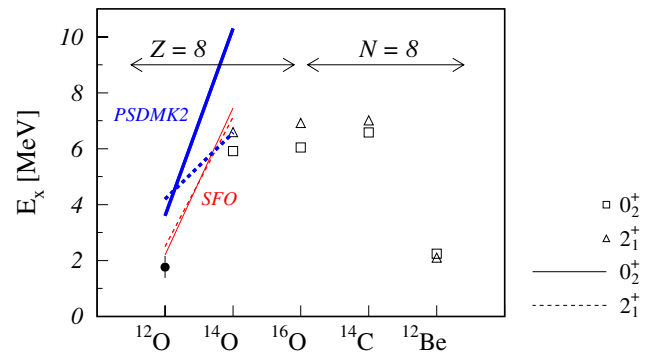


FIG. 4 (color online). Plot of E_x of the 2_1^+ and 0_2^+ states in the $Z = 8$ $^{12,14,16}\text{O}$ isotopes and $N = 8$ ^{12}Be and ^{14}C isotones. The shell-model predictions with the SFO (red, thin lines) and PSDMK2 (blue, bold lines) interactions [13] are shown together. The present result is denoted by the filled circle.

We then point out a notable similarity in the systematics between the isotopic chain with $Z = 8$ from ^{16}O to ^{12}O , and the isotonic chain with $N = 8$ from ^{16}O to ^{12}Be as shown in Fig. 4. In ^{12}Be , the lowering of E_x of the 2_1^+ and 0_2^+ states has indicated significant neutron sd -shell intruder configurations [13]. Thus, the lowered excited state in ^{12}O strongly suggests that the $Z = 8$ proton shell closure is also diminishing in ^{12}O . Indeed, the E_x of the state is found to be even smaller than those of the first excited states in other $N = 4$ isotones ^8Be and ^{10}C (2_1^+ at $E_x \sim 3$ MeV).

The observed breakdown of the proton shell closure in ^{12}O implies that the underlying mechanisms for the shell evolution prevail in the vicinity of the proton drip line. In the shell-model scheme, the advanced interaction with an enhanced proton-neutron monopole interaction (referred as SFO [13]) has well described the neutron shell quenching in ^{12}Be [13]. In neutron-rich nuclei around $N = 8$, the relative energy of the neutron $1p_{1/2}$ orbital is significantly changed by the presence or absence of protons in the $1p_{3/2}$ orbital, due to a strong attractive force between the two orbitals. Extending the concept to the proton-rich nuclei, one expects similar effects to persist in ^{12}O . Indeed, the structure change from ^{14}O to ^{12}O is explained by the same shell-model calculations with the SFO interaction as applied for ^{12}Be and ^{14}C [13], while the predictions of the PSDMK2 [13] interaction with a weaker monopole term show a large deviation at ^{12}O (Fig. 4). The large drop in E_x at ^{12}O can hardly be explained by the Coulomb shift only, where typical downward shifts for excited states are estimated to be 1 MeV or less [37]. The present observation thus suggests the important role of the proton-neutron monopole interaction as an isospin symmetric mechanism for shell evolution.

Apart from the shell model, several cluster models successfully describe the ^{12}Be structure [18,19], proposing the manifestation of a molecular structure such as $\alpha + \alpha + 4n$. In Refs. [18,19], the shell quenching is explained by a stabilization of the so-called “ σ -orbit” type molecular structure, which is realized at an optimal α - α distance of around 3 fm. It would be of great interest to investigate similar possibilities for ^{12}O with the $\alpha + \alpha + 4p$ structure, since one can naïvely expect that the additional repulsive Coulomb force leads to a rearrangement of the 2α configuration, and may degrade the stability of the cluster structure. The present results, however, clearly indicate mirror symmetry in the shell quenching, and thus serve as a stringent test for the role of the σ -orbit in the disappearance of the magic numbers 8.

In summary, we have identified a low-lying excited state in ^{12}O at 1.8(4) MeV using the $^{14}\text{O}(p, t)$ reaction. The lowering of the excitation energy indicates the breakdown of the shell closure at $Z = 8$. The mirror symmetry of the shell quenching phenomena in p -shell exotic nuclei is demonstrated, calling for a general representation of the nuclear shell structure and its evolution.

We thank the technical staff members of GANIL for their professional work. D.S. is grateful to the Japan Society for the Promotion of Science for support.

*Present address: NSCL, Michigan State University, USA.

- [1] M. Kobayashi and T. Maskawa, Prog. Theor. Phys. **49**, 652 (1973).
- [2] J. Bardeen, L. N. Cooper, and J. R. Schrieffer, Phys. Rev. **108**, 1175 (1957).
- [3] D. J. Lockwood *et al.*, Phys. Rev. Lett. **77**, 354 (1996).
- [4] Y. P. Chiu *et al.*, Phys. Rev. Lett. **97**, 165504 (2006).
- [5] D. E. Alburger *et al.*, Phys. Rev. C **17**, 1525 (1978).
- [6] H. Iwasaki *et al.*, Phys. Lett. B **491**, 8 (2000).
- [7] S. Shimoura *et al.*, Phys. Lett. B **560**, 31 (2003).
- [8] A. Navin *et al.*, Phys. Rev. Lett. **85**, 266 (2000).
- [9] S. D. Pain *et al.*, Phys. Rev. Lett. **96**, 032502 (2006).
- [10] T. Motobayashi *et al.*, Phys. Lett. B **346**, 9 (1995).
- [11] L. Gaudefroy *et al.*, Phys. Rev. Lett. **97**, 092501 (2006).
- [12] S. K. Tandel *et al.*, Phys. Rev. Lett. **97**, 082502 (2006).
- [13] T. Suzuki, R. Fujimoto, and T. Otsuka, Phys. Rev. C **67**, 044302 (2003).
- [14] T. Otsuka *et al.*, Phys. Rev. Lett. **95**, 232502 (2005).
- [15] G. A. Lalazissis *et al.*, Phys. Lett. B **418**, 7 (1998).
- [16] I. Hamamoto, Nucl. Phys. A **731**, 211 (2004).
- [17] H. Sagawa, B. A. Brown, and H. Esbensen, Phys. Lett. B **309**, 1 (1993).
- [18] N. Itagaki, S. Okabe, and K. Ikeda, Phys. Rev. C **62**, 034301 (2000).
- [19] Y. Kanada-En'yo, Phys. Rev. C **66**, 011303 (2002).
- [20] G. J. KeKelis *et al.*, Phys. Rev. C **17**, 1929 (1978).
- [21] S. Mordechai *et al.*, Phys. Rev. C **32**, 999 (1985).
- [22] R. A. Kryger *et al.*, Phys. Rev. Lett. **74**, 860 (1995).
- [23] P. Dolégiéviez *et al.*, Nucl. Instrum. Methods Phys. Res., Sect. A **564**, 32 (2006).
- [24] E. Pollacco *et al.*, Eur. Phys. J. A **25**, 287 (2005).
- [25] A. Joubert *et al.*, in *Proceedings of the Second Conference of the IEEE Particle Accelerator* (IEEE, New York, NY, 1991), p. 594.
- [26] L. Bianchi *et al.*, Nucl. Instrum. Methods Phys. Res., Sect. A **276**, 509 (1989).
- [27] S. Ottini-Hustache *et al.*, Nucl. Instrum. Methods Phys. Res., Sect. A **431**, 476 (1999).
- [28] GEANT4 Collaboration, Nucl. Instrum. Methods Phys. Res., Sect. A **506**, 250 (2003).
- [29] D. Suzuki, Doctoral thesis, University of Tokyo, 2009.
- [30] F. C. Barker, Phys. Rev. C **59**, 535 (1999).
- [31] L. V. Grigorenko *et al.*, Phys. Rev. Lett. **88**, 042502 (2002).
- [32] I. J. Thompson, Comput. Phys. Rep. **7**, 167 (1988).
- [33] N. Keeley *et al.*, Phys. Lett. B **646**, 222 (2007).
- [34] A. J. Koning and J. P. Delaroche, Nucl. Phys. A **713**, 231 (2003).
- [35] F. D. Becchetti and G. W. Greenlees, *Polarization Phenomena in Nuclear Reactions* (The University of Wisconsin Press, Madison, 1971).
- [36] D. Y. Pang *et al.*, Phys. Rev. C **79**, 024615 (2009).
- [37] H. T. Fortune and R. Sherr, Phys. Rev. C **74**, 024301 (2006).